Life Estimation for IC Plastic Packages Under Temperature Cycling Based on Fracture Mechanics

ASAO NISHIMURA, AKIHIRO TATEMICHI, HIDEO MIURA, AND TATSUJI SAKAMOTO

Abstract—**The strength of plastic encapsulants is analyzed from the viewpoint of crack propagation. With a preexisting crack length a and a specific number of applied load cycles N, fatigue crack propagation rates da/dN of the encapsulants were measured with laboratory test specimens. It was found that the da/dN of encapsulants can be expressed as functions of the stress intensity factor range ΔK. The crack propagation behavior in the package was estimated from the data of da/dN and ΔK at the lowest temperature of the test cycles. Reasonable correlation is found between the estimated crack propagation behavior and the observed one. The applicability of fracture mechanics to the package cracking problem is demonstrated.**

INTRODUCTION

RECENTLY, the size of integrated circuit chips mounted in plastic packages has been rapidly increasing, while the package dimensions have been restricted or even made smaller and thinner. This trend increases mechanical stress in the packages, which sometimes causes cracking in the plastic encapsulant (package cracking) during the development stage. Hence quantitative evaluation of the strength of encapsulants has become an important issue in the design of packages.

In the temperature cycling test of plastic encapsulated IC's, cracks in the encapsulant usually originate from the sharp edges of the chips or the lead frames. An illustration of the cross section of a cracked package is shown in Fig. 1, in which a crack originates from the lower edge of the chip pad. Since an extremely high concentration of stress exists around these sharp edges, the criteria for fracturing of the encapsulant at these points cannot be evaluated by the conventional approach based on maximum concentrated stress.

The curvature radii of edge tips are usually on the order of 1 μm and not controlled in the manufacturing process. Therefore, it is difficult to take account of curvature in the stress analysis of packages. If the finite element method is applied to the stress analysis of packages without considering edge tip curvature, the computed maximum stress value at the edge is dependent on the element size around the point and no definite values can be obtained. In this case, the edge tips are singular points within the elastic stress field, and it is meaningless to try to obtain maximum concentrated stress at these points.

Manuscript received February 11, 1987; revised July 15, 1987. This paper was presented at the 37th Electronic Components Conference, Boston, MA, May 11-13, 1987.

The authors are with Mechanical Engineering Research Laboratory, Hitachi, Ltd., 502 Kandatsu-machi, Tsuchiura, Ibaraki, 300 Japan.

IEEE Log Number 8717162.

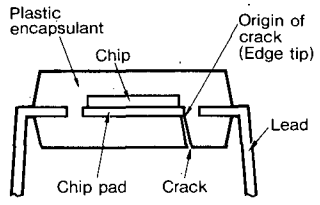

Fig. 1. Cross section of cracked package.

Even if the aforementioned stress can be obtained, the encapsulant strength with a high stress concentration cannot be determined by the maximum stress values alone. The results of bending tests for an encapsulant with sharp-notched plate specimens are shown in Fig. 2. The nominal fracture stress at the minimum cross section of the specimen and the maximum concentrated stress at fracture are plotted against the curvature of the notch tip. The data for zero curvature show those results with smooth specimens. Although the nominal fracture stress decreases with increasing curvature, the maximum concentrated stress of the notched specimens is far greater than the fracture stress of the smooth specimens. Therefore, some other parameters are required for the quantitative evaluation of the package cracking problem in place of the maximum concentrated stress.

In the temperature cycling test of packages, the length of cracks observed inside the packages gradually increases with the increasing number of temperature cycles [1]. This suggests that package cracking under temperature cycling is caused by encapsulant fatigue crack propagation. Fatigue crack propagation in most metallic materials has been successfully studied by using the linear fracture mechanics approach. If temperature cycles required for crack propagation can be estimated by assuming that small cracks already exist at the sharp edges, it will provide a conservative evaluation of the package reliability.

In this paper, linear fracture mechanics is applied to the package cracking problem, and the strength of the encapsulant is analyzed from the viewpoint of crack propagation. Fatigue crack propagation rates of encapsulants were measured using laboratory test specimens, and they were expressed as functions of stress intensity factor range ΔK, which is a measure of intensity of the stress singularity at the crack tip. The stress intensity factor K for package structure was analyzed as a function of the crack length, and the crack propagation life of the package was then estimated from these results.

0148-6411/87/1200-0637$01.00

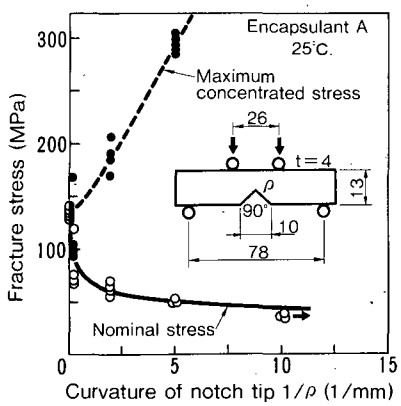

Fig. 2. Bending test results of sharp-notched specimen.

Temperature Cycling Tests of Experimental Packages

Temperature cycling tests of experimental packages were performed for the purpose of understanding the package cracking phenomenon. The packages used in the experiment were 600-mil dual inline packages with Alloy 42 lead frames molded with two different encapsulants. The combinations of the package type and the materials were selected to shorten the test period. Some thermal and mechanical properties of the encapsulants are listed in Table I. Both of the encapsulants are phenolic-cured epoxy resins filled with fused silica, but the thermal expansion coefficient of encapsulant A is lower than that of encapsulant B. Tests were performed between various temperature extremes, spending 20 min at each temperature extreme and 10 min in transition. The number of sample packages in each test condition was 20.

The results of the temperature cycling between -55 and $+150°C$ are shown in Fig. 3. The failure rates in this paper indicate the percentages of the packages which were found to have failed through visual inspection of the exterior surface. Most of the packages molded with encapsulant B failed within 200 cycles, while the packages with encapsulant A survived more than ten times longer than those with encapsulant B. All of the cracks observed in this study originated from the lower edge(s) of the chip pad and extended to the bottom surface of the package. In the case of the packages with encapsulant B, it was observed that initial cracks with a 0.1–0.3-mm length had already existed at the lower edges of both sides of the chip pad inside all the packages before the test. This means that the entire life of the packages with encapsulant B was spent for crack propagation. No initial cracks were observed in the packages with encapsulant A.

The effect of temperature conditions on the temperature cycling life of the packages molded with encapsulant B is shown in Fig. 4. The effect of the lowest temperature of the test cycles under constant temperature range is shown in Fig. 4(a), and the effect of the temperature range with the constantly lowest temperature is shown in Fig. 4(b). It can be seen from these figures that the temperature cycling life of the package is largely dependent on the lowest temperature of the cycles, where the thermal stresses become maximum during the cycles. The significance of the lowest temperature was also confirmed by monitoring the output of strain gauges bonded

TABLE I
THERMAL AND MECHANICAL PROPERTIES OF ENCAPSULANTS

Properties	Encapsulant A	Encapsulant B
Thermal expansion coefficient (1/°C)	18×10^{-6}	24×10^{-6}
Glass transition temperature (°C)	150	165
Young's modulus at 20°C (GPa)	15	15
Flexural strength at 20°C (MPa)	1.3×10^2	1.2×10^2
Fracture toughness at 20°C (MPa $\sqrt{m}$)	2.0	2.0

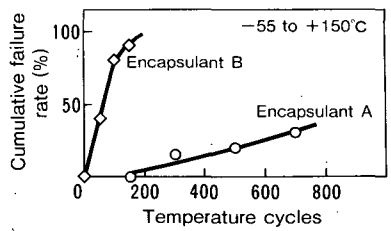

Fig. 3. Results of temperature cycling between $-55°C$ and $+150°C$.

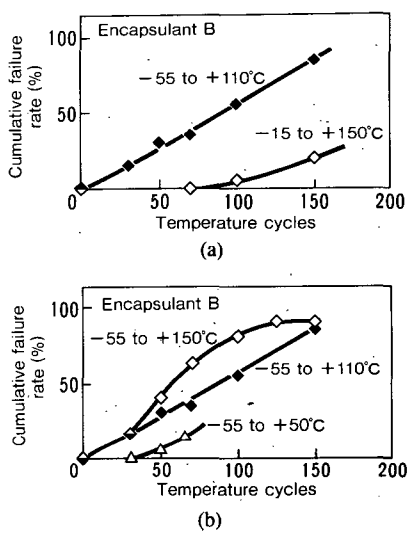

Fig. 4. Effect of temperature conditions on temperature cycling life of packages. (a) Effect of lowest temperature. (b) Effect of temperature range.

on the bottom surface of the package under temperature cycling. The amplitude of the gauge output gradually increased prior to crack penetration, and the output failed at the lowest temperature. These results indicate that the crack propagation in the package is mainly controlled by the lowest temperature of the test cycles.

Fatigue Crack Propagation Behavior of Encapsulants

Fatigue crack propagation rates of the two encapsulants in Table I were measured by the cycling tensile tests of single-edge-notched plate specimens. Dimensions of the specimens are shown in Fig. 5. Specimens were molded at 175°C and subsequently postcured at the same temperature for 5 h. A chevron notch was introduced with a diamond wafering blade 0.3 mm thick. Fatigue tests were performed using an electrohydraulic testing machine at -55, 25, and 150°C. The applied waveform was sinusoidal with constant load amplitude and stress ratios R (minimum–maximum load ratios) of 0 and 0.5. Crack propagation was monitored using foil crack gauges

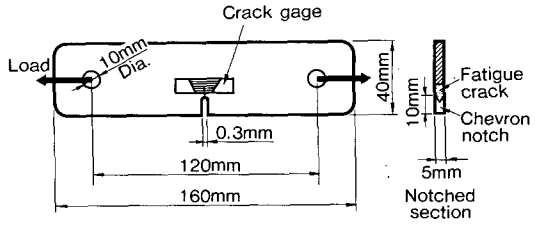

Fig. 5. Single-edge-notched specimen for fatigue crack propagation test.

bonded on the specimen's surfaces. The gauges have grids 0.2 mm apart, and crack propagation can be monitored as the change in electrical resistance. The crack propagation rates per cycle were plotted against the stress intensity factor range ΔK. The stress intensity factor range ΔK for the specimen was calculated by [2]

$$\Delta K=\frac{\Delta P\sqrt{a}}{Wt}\left\{1.99-0.41\frac{a}{W}+18.7\left(\frac{a}{W}\right)^2+38.48\left(\frac{a}{W}\right)^3+53.85\left(\frac{a}{W}\right)^4\right\} \quad (1)$$

where a is the crack length, ΔP is the range of applied load, W is the specimen width, and t is the specimen thickness.

The results for when the stress ratio R is 0 are shown in Fig. 6. The fatigue crack propagation rates da/dN are plotted on a logarithmically scaled graph against the stress intensity factor range ΔK. Cyclic frequencies of the tests at 25°C were varied from 0.02 to 10 Hz for both encapsulants, but little effect was recognized on the fatigue crack propagation rates. Therefore, da/dN for all the frequencies are plotted in Fig. 6 without distinction. The data for −55°C were measured at 1 and 10 Hz, and those for 150°C were at 10 Hz. It is shown that linear relationships exist between log da/dN and log ΔK at each temperature, and da/dN increases with the rise of the temperature. The linear relationships in Fig. 6 indicate that the fatigue crack propagation rates of encapsulants can be described by the well-known Paris relationship [3]

$$\frac{da}{dN}=C(\Delta K)^m \quad (2)$$

where a is the crack length, N is the number of cycles, and C and m are constants. Since the crack propagation rates are described as functions of ΔK, crack propagation behavior of the encapsulants under arbitrary conditions can be estimated if the ΔK is obtained.

The effect of the stress ratio R on the crack propagation rate of encapsulant A is shown in Fig. 7. The fatigue crack propagation rate of the encapsulant is greatly affected by the stress ratio. Assuming the same crack propagation rate in both cases, ΔK is 40 percent lower when $R = 0.5$ than when $R = 0$. Thus the temperature cycling test results in Fig. 4(a) are strongly dependent on the lowest temperature of the cycles, even when the span of the temperature range is the same.

The exponent m in (2), that is, the slope of each straight line in both Figs. 6 and 7, is around 20. This m value is much higher than that for most metallic materials, which is usually

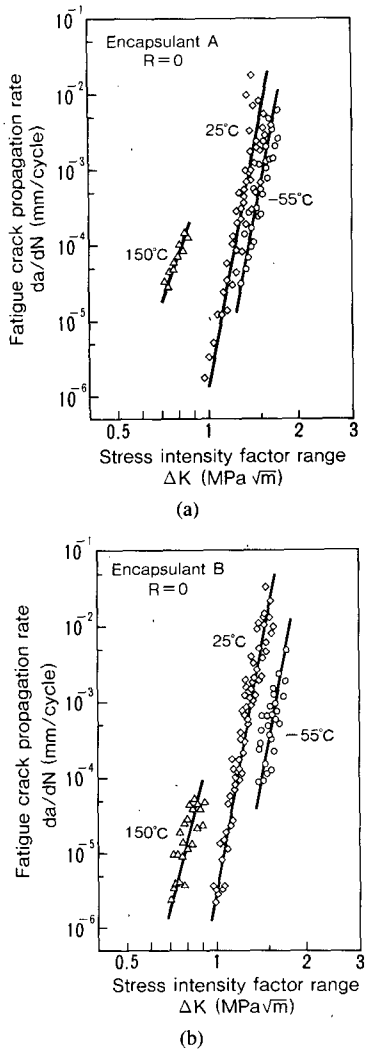

Fig. 6. Fatigue crack propagation rate of encapsulants. (a) Encapsulant A. (b) Encapsulant B.

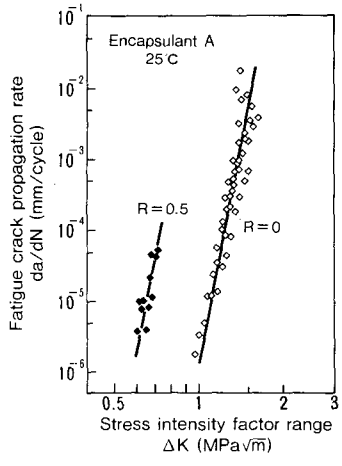

Fig. 7. Effect of stress ratio on fatigue crack propagation rate of encapsulant.

between two and eight. It means that the crack propagation rate of the encapsulant varies greatly, even with a slight change in ΔK.

Analysis of Stress Intensity Factor of Packages

The stress intensity factor K for the packages under temperature cycling was analyzed by means of the finite element method. The model for this analysis was the test package used in the experiment with package crack(s) extending from the side edge(s) of the chip pad towards the bottom surface of the package. Two types of crack propagation were considered: first, a single crack extending from one side of the chip pad; second, a pair of cracks symmetrically extending from both sides of the chip pad. Thermal stress analysis was performed on a transverse cross section of the package, assuming plane stress and linear elastic conditions. An example of the finite element mesh used in the analysis is shown in Fig. 8. Three-node triangular elements were used in this study. The stress intensity factor K was calculated from the values of the stress and the displacement of the crack tip elements using the equation proposed by Miyata *et al.* [4]. The direction of the crack extension was taken at an angle of 15° to the vertical, which was determined from experimental observation. The crack length was varied from 0.05 to 1.45 mm. The length of the sides of the smallest triangular elements around the crack was 10 μm for the crack length up to 0.23 mm and 50 μm for the larger crack length.

The interfaces of different materials were assumed to have perfect adhesion, except at the bottom surface of the chip pad. Stresses around the lower edges of the chip pad increase greatly with the delamination of the interface [5], and package cracking usually occurs under this condition. With regard to the test packages molded with encapsulant A, delamination was observed over the bottom surface of the chip pad within 10–20 cycles of temperature cycling between −55 and +150°C. The previous observation was made by means of ultrasonic inspection. The aforementioned number of temperature cycles is less than ten percent of the temperature cycles required for package cracking. As for the test packages with encapsulant B, perfect delamination was observed before temperature cycling. Therefore, it was assumed in this study that no adhesion existed between the bottom surface of the chip pad and the encapsulant from the beginning of the temperature cycling. The interfaces were assumed to slide against each other without friction.

Stress intensity factor K was analyzed for the temperature change from 150°C to −55°C. The encapsulant stress in the package is nearly zero at the glass transition temperature of the encapsulant and is almost proportional to the temperature difference from the glass transition temperature. As shown in Table I, the encapsulant glass transition temperatures are around 150°C. Hence it is assumed that encapsulant stress is zero at the highest temperature of the test cycles when temperature cycling is between −55°C and +150°C. The obtained stress intensity factor K at −55°C corresponds to the stress intensity factor range ΔK for the previous test condition.

The stress intensity factors for the test packages as functions of crack length a are shown in Fig. 9. The open symbols

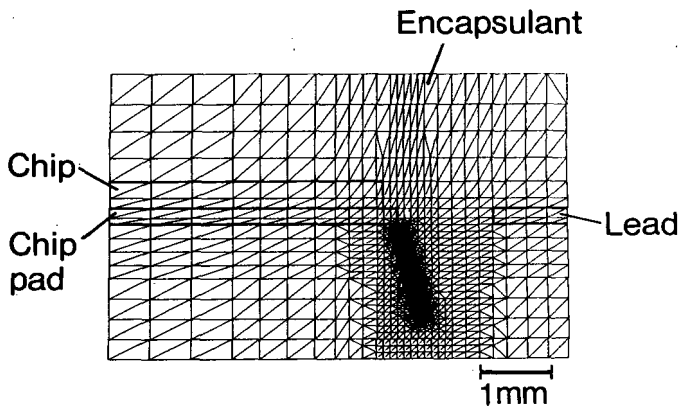

Fig. 8. Finite-element mesh for analysis of stress intensity factor of packages.

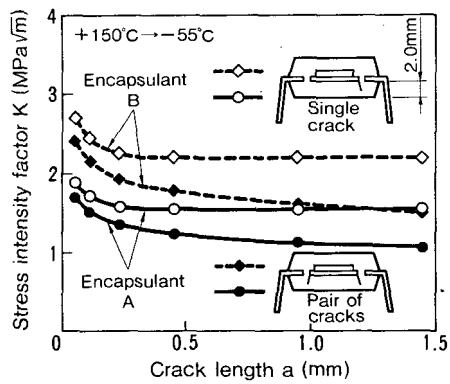

Fig. 9. Stress intensity factor for test packages.

represent the results for the single crack from one side of the chip pad, and the blackened ones represent those for the pairs of cracks symmetrically extending from both sides of the chip pad. It can be seen that the stress intensity factor K decreases rapidly as the crack length a increases up to about 0.2 mm and remains almost constant or decreases slightly for a larger crack length. The stress intensity factor for the packages molded with encapsulant A is about 30 percent lower than that for encapsulant B. The stress intensity factor becomes lower when cracks extend from both sides of the chip pad than when a single crack extends from one side of the chip pad. This is attributable to the absorption of the thermal shrinkage difference among the composing materials of the package by the opening deformation of the cracks. In the case of pairs of cracks, this thermal shrinkage difference is shared between the two cracks and thus the thermal stress in the package is relieved.

Estimation of Crack Propagation Life

Method of Estimation

In the temperature cycling test of packages, encapsulants are subjected to simultaneous fluctuation of both temperature and stress. As has been shown in Fig. 6, the strength of encapsulants, as well as thermal stress in the package, increase with decreasing temperature. However, since the thermal stress developing in the encapsulant is almost proportional to the temperature difference from the glass transition temperature of the encapsulant, its increase is more rapid than that of the strength. Therefore, the severity of the encapsulant's stress condition increases as the temperature of the package goes

down. This is supported by the experimental data in Fig. 4, where it was shown that the crack propagation in the package is mainly controlled by the lowest temperature of the test cycles. Hence it is considered that the crack propagation life of the package subjected to temperature cycling can be estimated from the data of da/dN and ΔK at the lowest temperature of the cycles.

The crack propagation life of the test packages can be estimated by substituting the relationships between K and the crack length a in Fig. 9 into (2) and performing the integration with respect to the crack length a. When the stress intensity factor range ΔK is represented by $\Delta K = f(a)$ as a function of crack length a, the number of temperature cycles required to propagate a crack from length a_0 to length a_c is given by

$$N = \int_{a_0}^{a_c} \frac{da}{Cf(a)^m} \tag{3}$$

where a_0 and a_c are the initial and final crack lengths, respectively.

The life was estimated for the temperature cycling between -55 and $+150$°C. Fatigue crack propagation rate data at $R = 0$ and -55°C were used in the estimation. The integration in (3) was performed numerically by representing $f(a)$ in a polynomial form. The initial crack length a_0 was taken to be 0.05 mm. Since the value of K and hence that of da/dN becomes large when the crack length is small as shown in Fig. 9, the value of a_0 has little effect on the integration results. This is provided that a_0 is taken to be less than about 0.1 mm. Crack propagation behavior in the package was estimated by varying the final crack length a_c in the integration up to 1.45 mm, which is about 70 percent of the thickness of the encapsulant under the chip pad. Although the crack propagation life in relation to the crack penetration was not estimated in this study, it is expected that the crack propagation will be accelerated as the crack tip approaches the bottom surface of the package, and the foregoing integration will provide an approximate estimation of the temperature cycling life.

Results of Estimation

The estimated results of the crack propagation behavior for the packages molded with encapsulant A are shown in Fig. 10. Crack propagation behavior for both the single crack from one side of the chip pad and the pair of cracks symmetrically extending from both sides of the chip pad were estimated. For comparison, experimental data are also plotted in Fig. 10. The experimental data for each point along the crack length were obtained by sectioning ten packages after predetermined temperature cycles and averaging the measured crack lengths. If observed cracks extended from both sides of the chip pad, the length of the longer crack was measured. It is shown that the temperature cycling life for the pair of cracks is far longer than that for the single crack, and the experimental data fall between the results of these two cases. There is little chance that cracks keep propagating from both sides of the chip pad to the bottom surface of the package completely symmetrically. The crack propagation in most of the encapsulant A packages was observed to be considerably asymmetric. The tendency of the estimated crack propagation behavior for the single crack

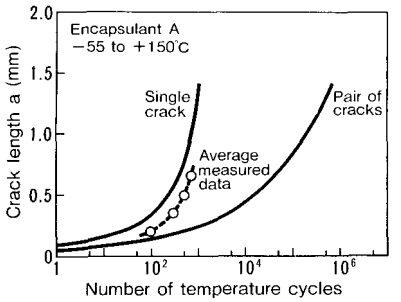

Fig. 10. Estimation of crack propagation behavior for test packages molded with encapsulant A.

correlates fairly well with that of the experimental data. Thus the applicability of the fracture mechanics to the package cracking problem is demonstrated.

The results for the packages with encapsulant B are shown in Fig. 11, with the experimental data obtained in the same manner. It is suggested that the estimated data for the single crack will lead to the final fracture of the package during the first cycle of the temperature cycling. In the case of encapsulant B packages, the initial cracks were observed extending from both sides of the chip pad inside all the packages before temperature cycling. Therefore, there was no package corresponding to the single crack model. It may be due to this fact that the experimental data in Fig. 11 are close to the estimated results for the pair of cracks at the early stages of crack propagation. The difference between the estimated crack propagation behavior and the experimental one at the later stages is probably due to the deviation of the crack propagation from the symmetric condition.

It was shown in Fig. 3 that some of the packages with encapsulant A failed between 300 and 700 cycles. The existence of these cracked packages cannot be predicted from the estimated results of Fig. 10. This suggests the necessity for further investigation. Since the fatigue crack propagation rate of the encapsulant varies greatly with a slight change in ΔK, as mentioned before, the estimated results are greatly affected by the accuracy of the stress intensity factor. For example, the scatter in package dimensions and material properties, the viscoelastic behavior of encapsulants, the three-dimensional effect of the package structure and other factors are considered to have a large effect on the stress intensity factors. Improving the accuracy of the estimation by taking account of these factors is a subject for future study.

Symmetry Effect of Crack Propagation

The symmetry effect of crack propagation on the temperature cycling life is also confirmed by the experimental data. The experimental data which show the symmetry effect of crack propagation on the life of the encapsulant B packages are shown in Fig. 12. The crack from one side of the chip pad was found to have reached the bottom surface of the package at a number of temperature cycles N. The length of the crack from the opposite side of the chip pad at that time is plotted against the number of temperature cycles N. The length of the embedded crack increases with the number of cycles N. Extended life of the package can be observed when the cracks on the opposing sides of the chip pad propagate at almost equal

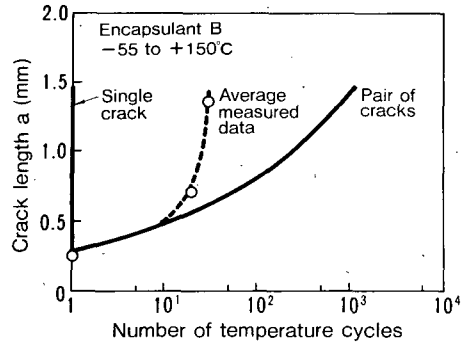

Fig. 11. Estimation of crack propagation behavior for test packages molded with encapsulant B.

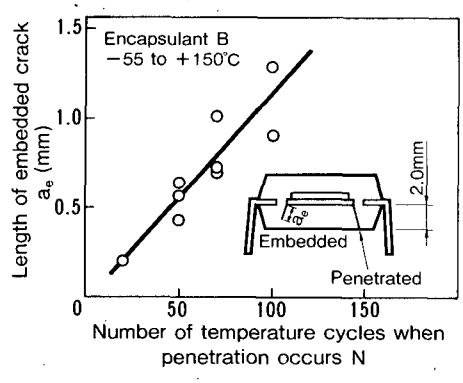

Fig. 12. Symmetry effect of crack propagation on temperature cycling life.

rates during temperature cycles. Note in Figs. 10–12 that the temperature cycling life of the package intrinsically varies over orders of magnitude even with equal package dimensions and equal material properties. The result of the present work points to the importance of symmetry in the design and the assemblage of packages.

Conclusion

The major results of this study can be summarized as follows. First, the results of the temperature cycling test of experimental packages suggest that the crack propagation in the package is mainly controlled by the lowest temperature of the test cycles. Second, the fatigue crack propagation rates da/dN of encapsulants can be described by $da/dN = C(\Delta K)^m$, which is a function of the stress intensity factor range ΔK. Third, the crack propagation behavior estimated from the data of da/dN and ΔK at the lowest temperature of the test cycles correlates fairly well with the experimental data. Fourth, the foregoing estimation indicates that the temperature cycling life of a package becomes far longer when cracks extend from both sides of the chip pad symmetrically than when a single crack extends from one side of the chip pad. This tendency was also confirmed by the experimental data.

Acknowledgment

The authors would like to thank Susumu Okikawa and Kunihiko Nishi for their helpful discussions.

References

[1] F. Shoraka, K. Kinsman, B. Natarajan, and C. Gealer, "Package and molding compound mechanics," in *Proc. 6th Ann. Int. Electronics Packaging Conf.*, 1986, pp. 294–312.

[2] B. Gross, J. E. Srawley, and W. F. Brown, Jr., "Stress intensity factors for a single edge-notch tension specimen by collocation of a stress function," NASA, Tech. Note D-2395, 1964.

[3] P. C. Paris and F. Erdogan, "A critical analysis of crack propagation laws," *Trans. ASME, Series D*, vol. 85, pp. 528–534, 1963.

[4] H. Miyata, S. Shida, and S. Kusumoto, "The simple method of evaluation of stress intensity factor using the finite element method," in *Proc. 1974 Symp. Mechanical Behavior of Materials*, 1974, The Society of Material Science, Japan, vol. 1, pp. 63–80.

[5] S. Groothuis, W. Schroen, and M. Murtuza, "Computer aided stress modeling for optimizing plastic package reliability," in *Proc. Int. Reliability Physics Symp.*, 1985, pp. 184–191.